DALTON
FULL PAPER

Solid-state luminescence and crystal structures of novel gold(I) benzenethiolate complexes

Seiji Watase,[a] Masami Nakamoto,*[a] Takayuki Kitamura,[b] Nobuko Kanehisa,[c] Yasushi Kai[c] and Shozo Yanagida*[b]

[a] *Osaka Municipal Technical Research Institute, Morinomiya, Joto-ku, Osaka 536-8553, Japan. E-mail: nakamoto@omtri.city.osaka.jp*
[b] *Material and Life Science, Graduate School of Engineering, Osaka University, Suita, Osaka 565-0871, Japan. E-mail: yanagida@chem.eng.osaka-u.ac.jp*
[c] *Department of Materials Chemistry, Graduate School of Engineering, Osaka University, Suita, Osaka 565-0871, Japan. E-mail: kai@chem.eng.osaka-u.ac.jp*

Received 9th August 2000, Accepted 23rd August 2000
First published as an Advance Article on the web 19th September 2000

A series of mononuclear bis(benzenethiolato)gold(I) complexes, $[n\text{-Bu}_4\text{N}][\text{Au}(\text{SC}_6\text{H}_4\text{R})_2]$ [R = H (**1**), *o*-Me (**2**), *o*-OMe (**3**), *o*-Cl (**4**), *m*-Me (**5**), *m*-OMe (**6**), *m*-Cl (**7**), *p*-Me (**8**), *p*-OMe (**9**) or *p*-Cl (**10**)] showed luminescence in the solid state at room temperature. The emission maxima ranged from 438 (blue emission) to 529 nm (green emission). The luminescence of these complexes is affected by substituent effects: electron-donating substituents (R = Me or OMe) on the benzene rings tend to shift the emission maxima toward shorter wavelengths, but the electron-withdrawing substituents (R = Cl) make the emission maxima shift toward longer wavelengths when compared to the maximum of the non-substituted species. This suggests that the luminescence properties could come from excited states due to a metal-to-ligand charge-transfer (MLCT) or ligand-centred (LC) transition. Complexes **2**, **4**, and **7** show normal linear S–Au–S geometries but exhibit no gold–gold interactions owing to the steric hindrance of the bulky counter cations, $[n\text{-Bu}_4\text{N}]^+$, which prevent the approach of two neighboring gold atoms. Both **2** and **4** show asymmetric configurations of the two thiolate ligands. On the other hand, **7** shows a completely symmetric configuration, where the gold atom is positioned at a center of symmetry.

Introduction

Much attention has been paid to the photophysical properties and photochemistry of gold(I) complexes with the closed shell electronic structure $[\text{Xe}]4f^{14}5d^{10}$. Since such gold(I) complexes exhibit intra- and/or inter-molecular d^{10}–d^{10} interactions and these may be an important factor for the luminescent behavior due to the metal-centered Au(5d)→Au(6p) transition, the preparation of polynuclear gold(I) complexes with gold–gold interactions has been conducted in the course of luminescence studies.[1–12] However, the luminescence of the binuclear gold(I) thiolate complex $[\text{Au}_2(p\text{-tc})_2(\text{dppe})]$ [*p*-tc = *p*-toluenethiolate; dppe = 1,2-bis(diphenylphosphino)ethane][13] and mononuclear gold(I) thiolate complexes $[\text{Au(SR)(PPh}_3)]$[14–17] and [Au(SR)-(TPA)] (TPA = 1,3,5-triaza-7-phosphaadamantanetriylphosphine)[15] has recently been assigned as arising from an S(π)→Au(6p) LMCT excited state. In addition, a binuclear gold(I) complex $[n\text{-Bu}_4\text{N}]_2[\text{Au}_2(i\text{-MNT})_2]$ (*i*-MNT = 1,1-dicyanoethylene-2,2-dithiolate)[18] and a trinuclear gold complex$[\text{Au(PEt}_3)_2][\text{Au(AuPEt}_3)_2(i\text{-MNT})_2]$[19] with a S–Au–S unit exhibited excited states as a result of S(π)→Au(6p) LMCT absorptions, giving luminescence. Those papers pointed out that the LMCT excited state originating from the S–Au–S unit is important for the luminescence, while the existence of π electrons of the phosphine ligand and intra- and/or inter-molecular gold–gold interactions may make it more complicated to estimate the contribution of the thiolate ligand to the luminescence behavior of those gold(I) thiolate complexes. Recently, we found that a series of mononuclear tetra-*n*-butylammonium bis(benzenethiolato)gold(I) complexes $[n\text{-Bu}_4\text{N}][\text{Au(SR)}_2]$ show solid-state luminescence. This type of complex offers an ideal luminescent gold system in terms of the following points: (i) the absence of phosphine ligands with π electrons, (ii) the presence of a bulky tetra-*n*-butylammonium cation $[n\text{-Bu}_4\text{N}]^+$, which may prevent gold–gold interaction in the solid state, and (iii) the ease of introduction of electron-donating or -withdrawing substituents on the benzenethiolate to study substituent effects on the luminescence.

In this paper we report the solid-state luminescence of a series of bis(benzenethiolato)gold(I) complexes, $[n\text{-Bu}_4\text{N}][\text{Au}(\text{SC}_6\text{H}_4\text{R})_2]$ [R = H (**1**), *o*-Me (**2**), *o*-OMe (**3**), *o*-Cl (**4**), *m*-Me (**5**), *m*-OMe (**6**), *m*-Cl (**7**), *p*-Me (**8**), *p*-OMe (**9**) or *p*-Cl (**10**)] and the crystal structures of **2**, **4**, and **7** with no gold–gold interactions in the crystals. All the complexes luminesce in the solid state and also exhibit characteristic substituent effects on the luminescence, suggesting an MLCT or LC transition rather than an LMCT one.

Results and discussion

Luminescence

The present bis(benzenethiolato)gold(I) complexes except complex **4** (luminesces at 77 K) show bright luminescence in the solid state at room temperature, as depicted in Fig. 1. The solid-state absorption (KBr method), excitation, and emission wavelengths of **1**–**10** are summarized in Table 1. The solid-state absorption and excitation spectra of **7** are shown in Fig. 2. Complex **7** displays broad and intense absorption in the range 250 to 350 nm and the maximum is at 292 nm (ε 18000 $\text{dm}^3\ \text{mol}^{-1}\ \text{cm}^{-1}$), while there appear no significant absorptions at wavelengths greater than 350 nm. All other gold(I) thiolate complexes also afford similar absorptions in the same region.

In the literature,[16] absorption of $[\text{AuX(PR}_3)]$ (R = Ph or Et; X = L-cysteinate or thiomalate) at *ca.* 290 and 360 nm are assigned to S→Au charge-transfer transitions on the basis of

Table 1 Luminescence data of bis(benzenethiolato)gold(I) complexes

Complex	Absorption[a] λ_{max}/nm (ε)[b]	Excitation[c] λ_{max}/nm	Emission[c] λ_{max}/nm
1 [*n*-Bu_4N][Au(SC_6H_5)$_2$]	287 (19000)	350	501
2 [*n*-Bu_4N][Au(SC_6H_4Me-*o*)$_2$]	285 (17000)	336	469
3 [*n*-Bu_4N][Au(SC_6H_4OMe-*o*)$_2$]	280 (14000)	342	450
4 [*n*-Bu_4N][Au(SC_6H_4Cl-*o*)$_2$]	290 (18000)	No luminescence	
5 [*n*-Bu_4N][Au(SC_6H_4Me-*m*)$_2$]	287 (17000)	326	482
6 [*n*-Bu_4N][Au(SC_6H_4OMe-*m*)$_2$]	283 (17000)	353	480
7 [*n*-Bu_4N][Au(SC_6H_4Cl-*m*)$_2$]	292 (18000)	386	512
8 [*n*-Bu_4N][Au(SC_6H_4Me-*p*)$_2$]	286 (16000)	370	489
9 [*n*-Bu_4N][Au(SC_6H_4OMe-*p*)$_2$]	283 (19000)	355	438
10 [*n*-Bu_4N][Au(SC_6H_4Cl-*p*)$_2$]	296 (19000)	367	529

[a] Solid-state absorption spectra were measured in KBr. [b] Molar absorption coefficient ($dm^3\ mol^{-1}\ cm^{-1}$) calculated from the volume and thickness of the KBr disk. [c] Solid-state excitation and emission spectra were measured at 298 K.

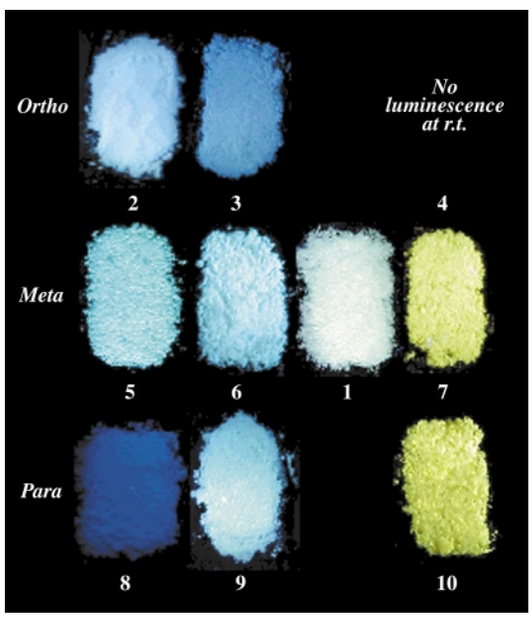

Fig. 1 Photograph of the luminescence of [*n*-Bu_4N][Au(SC_6H_4R)$_2$] [R = H(**1**), *o*-Me (**2**), *o*-OMe (**3**), *o*-Cl (**4**), *m*-Me (**5**), *m*-OMe (**6**), *m*-Cl (**7**), *p*-Me (**8**), *p*-OMe (**9**) or *p*-Cl (**10**)] excited by the xenon lamp.

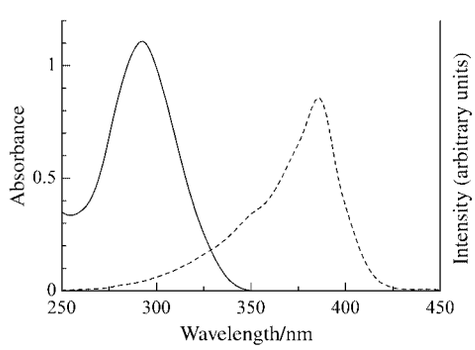

Fig. 2 Solid-state absorption (—) and excitation (– – –) spectra of complex **7**.

UV-visible and CD spectra and SCF-MO calculations. Analogous gold(I) complexes containing the toluenethiolate ligand, [Au(PR_3)(SC_6H_4Me-*p*)] (R = Me or Ph) and [Au_2(dppm)-(SC_6H_4Me-*p*)$_2$] [dppm = bis(diphenylphosphino)methane], were reported to show absorptions at 260 and 280 nm, which are mainly composed of intraligand (IL) transitions of *p*-toluenethiolate with additional charge transfer or metal-centered transitions in the region 300 to 330 nm on the basis of Gaussian band spectral fitting.[17] Thus, the similarities in peak positions and absorptivities of the present gold(I) thiolate

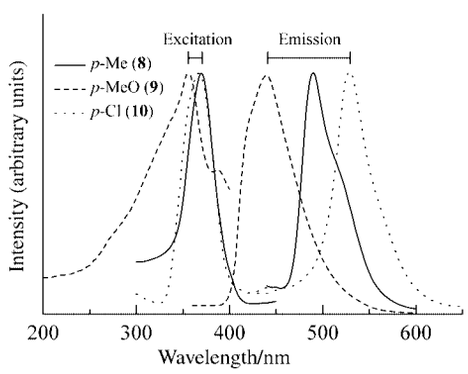

Fig. 3 Solid-state excitation and emission spectra of complexes **8**–**10**.

complexes to those of [Au(PR_3)(SC_6H_4Me-*p*)] (R = Me or Ph) may lead to the assignment of the intense 290 nm absorption bands of the present complexes mainly as IL transitions of the thiolate ligands.

Complex **7** shows solid-state luminescence (λ_{em} = 512 nm) upon excitation at 386 nm at room temperature. Similarly, intense emissions ranging from 438 to 529 nm were recorded for the other complexes upon excitation at 326–386 nm, respectively, as shown in Table 1. In the region of excitation there exist no obvious absorptions for the present complexes in the solid state (Fig. 2) and in solution. However, at higher concentrations in acetonitrile solution (2.4×10^{-2} mol dm^{-3}), quite weak shoulders (ε 10 $dm^3\ mol^{-1}\ cm^{-1}$) appear to lower energy (350–420 nm), the wavelengths of which are compatible with those of the observed excitation.† Thus, it suggests that the excitation of the present complexes could come from an intrinsic forbidden transition in this region rather than the stronger high-energy transitions at *ca.* 290 nm.

The solid-state excitation spectra of complexes **8**–**10** in Fig. 3 were observed in the narrow range from λ_{ex} = 355 to 370 nm. Such behavior is suggestive of the excitation based on the same origin in complexes **8**–**10**. On the other hand, the emission of these complexes showed very large Stokes shifts (>5000 cm^{-1}), and the emission maxima appeared over a wide range from λ_{em} = 438 nm (blue emission) to 529 nm (green emission) in spite of the narrow range of the excitation wavelengths. Similar results were obtained for complexes **1**–**7** (Table 1). Large Stokes shifts of 83–177 nm (5300–9900 cm^{-1}) between the excitation and emission wavelengths for each complex suggest that a large distortion occurs in the excited state, based on the electronic and/or steric effect of the substituents on the benzene rings. These results prompted us to study substituent effects on the emission spectra.

† Despite the observation of weak transitions responsible for the luminescence at higher concentrations in solution, all the complexes are not luminescent in solution at room temperature.

Compared to the emission maximum (λ_{em} = 501 nm) of the non-substituted benzenethiolate complex **1**, electron-donating substituents such as methyl or methoxy on the thiolate ligands cause the emission maxima to shift 12–63 nm toward shorter wavelengths (blue shift). On the other hand, the electron-withdrawing chloro group causes the emission maximum to shift 19–28 nm to longer wavelengths (red shift). Furthermore, the emission maxima shift to the longer wavelengths in the order OMe < Me < (H) < Cl in spite of the *ortho*, *meta*, and *para* positions of substituents. This reveals that the electronic property of the substituent reflects the emission behavior induced by the same excitation process for all the complexes described. It should be noted that the difference of the emission maxima, $\Delta\lambda_{em}$ = 91 nm (3900 cm^{-1}), in the series of *para* substituted derivatives **8**–**10** is much greater than the values for the *ortho* [$\Delta\lambda_{em}$ = 51 nm (2200 cm^{-1})] and *meta* derivatives [$\Delta\lambda_{em}$ = 40 nm (1600 cm^{-1}). In practice, complex **9** with *p*-OMe and complex **10** with *p*-Cl show blue and yellowish green emission, respectively (Fig. 1). Such a color change is reasonably explained by the resonance effect of the benzene ring, which amplifies the normal electronic effects of substituent on the thiolate ligand.

It is well known that substituents on a ligand affect the excitation and emission spectra due to an LMCT transition;[20] the electron-withdrawing substituents of previous reported gold(I) phosphine thiolate complexes, [Au(SR)(TPA)] (SR = SC_6H_4X; X = H, OMe or Cl), cause a blue shift of the emission energy compared to that of the unsubstituted one, and electron-donating substituents and/or the formation of intermolecular gold–gold interactions result in a red shift.[15] In addition, changing a *p*-toluenethiolate (*p*-tc) ligand of [Au_2(*p*-tc)$_2$(dppe)] to the more electron donating propanedithiolate ligand also causes a red shift in the emission energy.[13] However, the opposite trend of the substituent effects on the excitations and emissions was observed in this study as described above. Such a substituent dependence of the emission rules out LMCT processes, although the previously reported gold(I) thiolate complexes luminesce due to LMCT transitions.[13–19,21] The metal-centered transition arising from the gold–gold contacts can also be disregarded, since complexes **2**, **4**, and **7** form no gold–gold interactions in the crystals as described in the section Crystal structures. Therefore, the possible sources of excitations in this work may be a metal-to-ligand charge transfer transition from gold (5d) to ligand (π*) or a ligand-centered (LC) transition from sulfur (non-bonding 3p) to the benzene ring (π*) of the benzenethiolate ligand.

Gold(I) centers in the present bis-thiolate complexes may have more electron-rich circumstances than those of the gold(I) phosphine thiolate complexes, inducing elevation of the metal orbitals level so as to make the π* orbital of the ligand an acceptor.[21] Thus, the luminescent behavior of the present complexes may reasonably be explained by an MLCT excitation; an electron-withdrawing substituent on the ligand lowers the ligand orbitals (π*), which may result in a red shift of the emission. Conversely, an electron-donating substituent may cause a blue shift of the emission. On the other hand, an LC transition is another candidate, because the emission is also expected to occur from a π* excited state. Therefore, the emission origin of bis(benzenethiolato)gold(I) complexes may provisionally be assigned to an MLCT or LC transition. Furthermore, the weakness of the absorption process does suggest a spin-forbidden excited state such as ^{3}MLCT or ^{3}LC being responsible, which are induced by the relativistic effect of the heavy gold atom,[9,22–25] but this is tentative.

Crystal structures

The crystal structures of the complexes [*n*-Bu_4N][Au(SC_6H_4-R)$_2$] [R = *o*-Me (**2**), *o*-Cl (**4**), or *m*-Cl (**7**)] have been determined by single crystal X-ray diffraction. Selected bond lengths and angles are listed in Table 2.

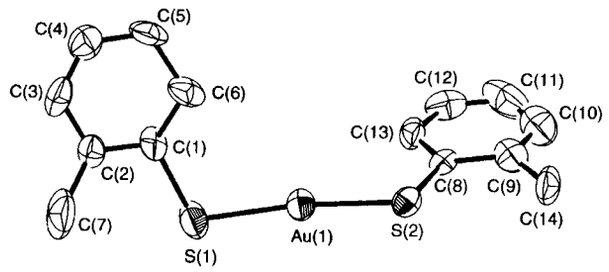

Fig. 4 An ORTEP[26] view of complex **2**. Thermal ellipsoids (in all cases) are drawn at the 30% probability level.

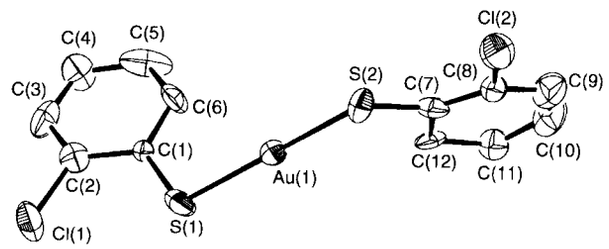

Fig. 5 An ORTEP view of complex **4**.

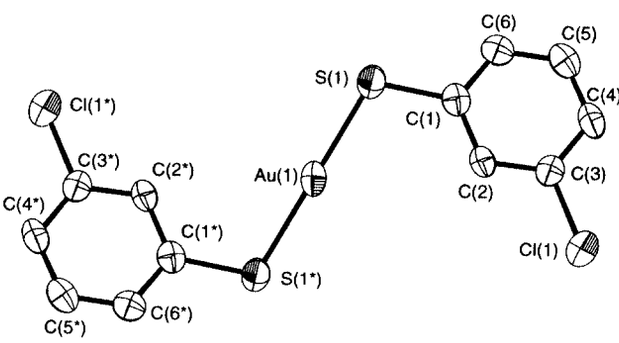

Fig. 6 An ORTEP view of complex **7**.

The anionic part of complex **2** contains an asymmetric structure as shown in Fig. 4. Complex **2** shows a linear S–Au–S geometry with the angle S(1)–Au(1)–S(2) 172.7(1)°, which is comparable to values in previously reported bis(thiolato)gold(I) complexes ranging from 175.11(5) to 178.8(2)°.[27–30] The two Au–S bond lengths are slightly different from each other [2.292(9) and 2.256(8) Å], but lie in the normal range for mononuclear complexes of this type [2.251(6)–2.288(4) Å].[27–30] The two S–C bond lengths [1.85(2) and 1.71(2) Å] correspond to a single bond (1.82 Å).[31] The gold atoms in neighboring molecules are separated by 8.492 Å and there exists no gold–gold interaction in the crystal of complex **2**. This result is explained by the steric hindrance of the bulky tetra-*n*-butylammonium cation (see below). The Au(1)–S(1)–C and Au(1)–S(2)–C bond angles are 108.8(8) and 111.8(8)°, respectively, and the two thiolate ligands are located asymmetrically (Fig. 4).

The X-ray analysis of complex **4** with chloro-substituent at the *ortho* position of the benzene ring gave similar results regarding the basic S–Au–S moiety and the asymmetric configuration of the thiolate ligand as shown in Fig. 5. On the other hand, complex **7** shows a completely symmetric structure with S(1)–Au(1)–S(1*) 180.0°, where the gold atom in the anionic part of the complex is located at a crystallographic center of symmetry and the two benzenethiolate planes are parallel to each other (Fig. 6). This is the first example of a bis(thiolato)-gold(I) complex with a completely symmetric structure.

In spite of the difference of the symmetry in the ligand configurations, the crystal packing diagrams of these complexes show the insertion of tetra-*n*-butylammonium cations into the arrangement formed by the anionic parts. Based on these clear-cut crystal packings, the steric hindrance of the bulky counter cation, $[n\text{-}Bu_4N]^+$, apparently prevents the formation of intermolecular gold–gold interactions as we expected. Thus, the crystal structures of these complexes **2**, **4**, and **7** exclude solid-state luminescence based on metal-centered transitions derived from gold–gold interactions for the present luminescent complexes.

Table 2 Selected bond lengths (Å) and angles (°) for complexes **2**, **4** and **7**

	o-Me (**2**)	*o*-Cl (**4**)	*m*-Cl (**7**)
Au(1)–S(1)	2.292(9)	2.282(12)	2.288(2)
Au(1)–S(2)	2.256(8)	2.284(12)	
S(1)–C	1.85(2)	1.73(3)	1.766(8)
S(2)–C	1.71(2)	1.78(3)	
Au · · · Au	8.492(1)	8.562(3)	8.348(2)
S–Au(1)–S	172.7(1)	172.1(2)	180.0
Au(1)–S(1)–C	108.8(8)	109.3(9)	108.9(3)
Au(1)–S(2)–C	111.8(8)	110.6(10)	

Conclusion

Mononuclear bis(benzenethiolato)gold(I) complexes **1**–**10** have been prepared. Luminescent properties of the present d^{10}-gold(I) complexes in the solid state at room temperature are characterized by MLCT or LC transitions. The substituents on the benzene rings shift the emission maxima toward longer wavelengths in the order MeO < Me < (H) < Cl. In the case of *para* substituted derivatives, the resonance effect of the benzene ring as well as the electronic effect of the substituent on the thiolate ligand reflect the emission behavior. Ligand control

Table 3 Analytical data for bis(benzenethiolato)gold(I) complexes

Complex	Yield (%)	mp/°C	Found (Calc.) %C	%H	%N	Far-IR (300–700 cm^{-1})	^1H NMR (δ)	^{13}C-{^1H} NMR(δ)
1	74	66.5–67.5	50.89 (51.13)	6.91 (7.05)	2.15 (2.13)	429, 478, 696	0.92 (t, 12H), 1.33 (m, 8H), 1.45 (m, 8H), 3.06 (t, 8H), 6.88 (t, 2H), 6.99 (t, 4H), 7.60 (d, 4H)	13.7, 19.7, 24.0, 58.8, 122.2, 127.6, 131.9, 144.9
2	78	91.5–92.5	52.24 (52.54)	7.07 (7.35)	2.06 (2.04)	371, 391, 439, 454, 554, 676	0.92 (t, 12H), 1.33 (m, 8H), 1.43 (m, 8H), 2.41 (s, 6H), 3.04 (t, 8H), 6.81 (m, 4H), 6.98 (d, 2H), 7.98 (d, 2H)	13.7, 19.7, 22.5, 24.0, 58.8, 122.4, 124.7, 129.4, 134.0, 137.8, 144.2
3	73	98.0–99.5	49.92 (50.20)	6.92 (7.02)	2.03 (1.95)	372, 421, 452, 501, 575, 679	0.92 (t, 12H), 1.35 (m, 8H), 1.52 (m, 8H), 3.15 (t, 8H), 3.84 (s, 6H), 6.67 (m, 4H), 6.85 (t, 2H), 8.03 (d, 2H)	13.7, 19.7, 24.0, 55.8, 58.9, 110.5, 119.8, 123.2, 133.2, 135.2, 158.1
4	64	105.5–106.5	46.05 (46.28)	5.89 (6.10)	2.00 (1.93)	336, 436, 448, 472, 488, 660	0.91 (t, 12H), 1.33 (m, 8H), 1.50 (m, 8H), 3.10 (t, 8H), 6.80 (t, 2H), 6.91 (t, 2H), 7.18 (d, 2H), 8.10 (d, 2H)	13.7, 19.7, 24.0, 58.9, 123.4, 125.4, 129.1, 134.1, 135.3, 143.9
5	72	71.5–73.0	52.30 (52.54)	7.39 (7.35)	2.08 (2.04)	342, 418, 430, 440, 525, 679, 693	0.91 (t, 12H), 1.32 (m, 8H), 1.45 (m, 8H), 2.19 (s, 6H), 3.07 (t, 8H), 6.67 (d, 2H), 6.88 (t, 2H), 7.38 (d, 2H), 7.43 (s, 2H)	13.7, 19.7, 21.4, 24.0, 58.7, 123.1, 127.5, 129.0, 132.6, 137.0, 144.5
6	75	43.0–45.0	49.78 (50.20)	7.01 (7.02)	2.01 (1.95)	356, 382, 426, 445, 566, 590, 684	0.93 (t, 12H), 1.34 (m, 8H), 1.48 (m, 8H), 3.10 (t, 8H), 3.71 (s, 6H), 6.44 (d, 2H), 6.90 (t, 2H), 7.20 (m, 4H)	13.7, 19.7, 24.0, 55.1, 58.8, 108.3, 117.1, 124.7, 128.2, 146.3, 158.9
7	80	69.5–70.5	46.16 (46.28)	6.05 (6.10)	1.94 (1.93)	301, 395, 420, 433, 443, 663, 679	0.93 (t, 12H), 1.34 (m, 8H), 1.48 (m, 8H), 3.06 (t, 8H), 6.84 (d, 2H), 6.93 (t, 2H), 7.44 (d, 2H), 7.57 (s, 2H)	13.7, 19.8, 24.0, 58.8, 122.3, 128.7, 130.0, 131.0, 133.0, 147.5
8	69	87.0–88.0	52.50 (52.54)	7.31 (7.35)	2.12 (2.04)	388, 395, 407, 413, 489, 495, 626	0.92 (t, 12H), 1.33 (m, 8H), 1.45 (m, 8H), 2.21 (s, 6H), 3.08 (t, 8H), 6.80 (d, 4H), 7.47 (d, 4H)	13.7, 19.7, 20.8, 24.0, 58.8, 128.4, 131.3, 131.8, 140.8
9	77	64.0–65.5	49.85 (50.20)	6.96 (7.02)	2.07 (1.95)	334, 378, 399, 513, 625, 638	0.93 (t, 12H), 1.34 (m, 8H), 1.48 (m, 8H), 3.10 (t, 8H), 3.71 (s, 6H), 6.60 (d, 4H), 7.47 (d, 4H)	13.7, 19.8, 24.1, 55.4, 58.8, 113.5, 132.8, 134.9,156.1
10	48	67.0–68.0	46.02 (46.28)	5.95 (6.10)	2.06 (1.93)	485, 494, 541	0.95 (t, 12H), 1.36 (m, 8H), 1.51 (m, 8H), 3.10 (t, 8H), 6.96 (d, 4H), 7.52 (d, 4H)	13.7, 19.8, 24.0, 58.9, 127.5, 127.9, 133.0, 143.3

Table 4 Crystal data, data collection, and structure refinement for complexes **2**, **4** and **7**

	o-Me (**2**)	*o*-Cl (**4**)	*m*-Cl (**7**)
Chemical formula	$C_{30}H_{50}AuNS_2$	$C_{28}H_{44}AuCl_2NS_2$	$C_{28}H_{44}AuCl_2NS_2$
Formula weight	685.82	726.65	726.65
Crystal system	Monoclinic	Monoclinic	Monoclinic
Space group	*Cc* (no. 9)	*Cc* (no. 9)	*C*2/*c* (no. 15)
a/Å	14.222(2)	14.191(3)	23.427(4)
b/Å	13.923(2)	13.549(5)	8.938(4)
c/Å	16.953(2)	17.109(3)	16.696(4)
β/°	109.17(1)	108.68(1)	118.01(1)
V/Å^3	3171(1)	3116(1)	3086(1)
Z	4	4	4
T/°C	23.0	23.0	23.0
μ(Mo-Kα)/cm^{-1}	48.05	50.60	51.08
No. of measured reflections	3773	3723	3624
No. of unique reflections	3631	3566	3542
R_{int}	0.048	0.112	0.026
R (R_w)	0.040 (0.025)	0.080 (0.035)	0.035 (0.029)

for the present bis(benzenethiolato)gold(I) complexes has effected a color change of the emission. Complexes **2**, **4**, and **7** crystallize in the monoclinic space groups *Cc*(no. 9), *Cc*(no. 9) and *C*2/*c*(no. 15), respectively. All these complexes include normal linear S–Au–S geometries, but exhibit no gold–gold interactions owing to the steric hindrance of the bulky tetra-*n*-butylammonium counter cations.

Experimental

All experiments were carried out under a nitrogen atmosphere by using standard Schlenk techniques. Commercially available tetrachloroauric acid, $HAuCl_4 \cdot 4H_2O$, and benzenethiols were used without further purification. Triethylamine was purified by distillation. Tetrahydrofuran (THF) as a reaction solvent was distilled over CaH_2 under a nitrogen atmosphere before use. Tetra-*n*-butylammonium dibromoaurate(I), [*n*-Bu_4N][$AuBr_2$], was prepared by the literature method.[32]

Syntheses

The bis(benzenethiolato)gold(I) complexes, **1**–**10** were prepared by a modification of the literature method;[32] [*n*-Bu_4N][$AuBr_2$] was allowed to react with two equivalents of the corresponding benzenethiols ArSH in the presence of triethylamine as a base,[14] (eqn. 1). All the complexes were readily isolated in high

$$[n\text{-}Bu_4N][AuBr_2] + 2\ ArSH + 2\ Et_3N \longrightarrow [n\text{-}Bu_4N][Au(SAr)_2] + 2\ Et_3NHBr \quad (1)$$

yields (Table 3) and can be crystallized from methanol to yield colorless crystals. The resulting single crystals of the complexes **2**, **4**, and **7** were found suitable for X-ray crystallographic analysis.

[*n*-Bu_4N][$Au(SC_6H_5)_2$] 1. A mixture of benzenethiol (0.37 g, 3.3 mmol) and triethylamine (0.34 g, 3.3 mmol) in THF (20 cm^3) was added dropwise to a solution of [*n*-Bu_4N][$AuBr_2$] (1.00 g, 1.7 mmol) in the same solvent (10 cm^3) and stirred for 2 h at room temperature. A white precipitate of Et_3NHBr was filtered off and the THF evaporated under reduced pressure to give a white residue. This was triturated with diethyl ether (3 cm^3) two times, the solvent removed, and then the residue dried *in vacuo*. The product was purified by recrystallization from methanol to give colorless crystals of [*n*-Bu_4N][Au-(SC_6H_5)$_2$] **1** in 74% yield. Analytical and spectroscopic data are shown in Table 3.

Instrumentation

Elemental analyses were performed on a Yanaco MT-3 CHN corder. ^{1}H and ^{13}C{^{1}H} NMR spectra were collected on a JEOL JNM-EX270 Spectrometer in $CDCl_3$ by the use of tetramethylsilane as an internal standard, far-infrared spectra from KBr pellets on a Perkin-Elmer spectrum GX-I0 FT-IR system, UV-Visible absorption spectra on a Shimadzu UV-265FW spectrophotometer and emission and excitation spectra on a Shimadzu RF-5000 spectrofluorophotometer equipped with an OXFORD DN1754 cryostat and an ITC4 intelligent temperature controller using a xenon lamp as the excitation source.

Crystallography

Colorless single crystals of the complexes **2**, **4**, and **7** were mounted on glass fibers with epoxy resin. Intensity data were collected on a Rigaku AFC-5R four-circle diffractometer with graphite-monochromated Mo-Kα radiation and the ω–2θ scan mode. They were corrected for decay and Lorentz-polarization effects, and empirical absorption corrections were made based on the φ scans. The structures were solved by direct methods[34] and expanded using Fourier techniques.[35] The non-hydrogen atoms were refined anisotropically, while atoms C(1) and C(11) of complex **4** were refined isotropically. Hydrogen atoms were placed in calculated positions (C–H 0.95 Å) but not refined. The final cycle of full-matrix least-squares refinement was based on observed reflections and variable parameters. All calculations were performed using the TEXSAN crystallographic software package.[36]

CCDC reference number 186/2155.

See http://www.rsc.org/suppdata/dt/b0/b006572m/ for crystallographic files in .cif format.

References

1 C. King, J.-C. Wang, M. N. I. Khan and J. P. Fackler, Jr., *Inorg. Chem.*, 1989, **28**, 2145.
2 C.-M. Che, H.-L. Kwong, V. W.-W. Yam and K.-C. Cho, *J. Chem. Soc., Chem. Commun.*, 1989, 885.
3 C.-M. Che, H.-L. Kwong, C.-K. Poon and V. W.-W. Yam, *J. Chem. Soc., Dalton Trans.*, 1990, 3215.
4 V. W.-W. Yam, T.-F. Lai and C.-M. Che, *J. Chem. Soc., Dalton Trans.*, 1990, 3747.
5 D. Perreault, M. Drouin, A. Michel and P. D. Harvey, *Inorg. Chem.*, 1991, **30**, 2.
6 D. Li, C.-M. Che, S.-M. Peng, S.-T. Liu, Z.-Y. Zhou and T. C. W. Mak, *J. Chem. Soc., Dalton Trans.*, 1993, 189.
7 V. W.-W. Yam and W.-K. Lee, *J. Chem. Soc., Dalton Trans.*, 1993, 2097.
8 V. W.-W. Yam and S. W.-K. Choi, *J. Chem. Soc., Dalton Trans.*, 1994, 2057.
9 Z. Assefa, B. G. McBurnett, R. J. Staples and J. P. Fackler, Jr., *Inorg. Chem.*, 1995, **34**, 4965.
10 S. S. Tang, C.-P. Chang, I. J. B. Lin, L.-S. Liou and J.-C. Wang, *Inorg. Chem.*, 1997, **36**, 2294.

11 H. Xiao, Y.-X. Weng, W.-T. Wong, T. C. W. Mak and C.-M. Che, *J. Chem. Soc.*, *Dalton Trans.*, 1997, 221.
12 M. Bardají, A. Laguna, V. M. Orera and M. D. Villacampa, *Inorg. Chem.*, 1998, **37**, 5125.
13 W. B. Jones, J. Yuan, R. Narayanaswamy, M. A. Young, R. C. Elder, A. E. Bruce and M. R. M. Bruce, *Inorg. Chem.*, 1995, **34**, 1996.
14 M. Nakamoto, W. Hiller and H. Schmidbaur, *Chem. Ber.*, 1993, **126**, 605.
15 J. M. Forward, D. Bohmann, J. P. Fackler, Jr. and R. J. Staples, *Inorg. Chem.*, 1995, **34**, 6330.
16 D. H. Brown, G. Mckinlay and W. E. Smith, *J. Chem. Soc.*, *Dalton Trans.*, 1977, 1874.
17 R. Narayanaswamy, M. A. Young, E. Parkhurst, M. Ouellete, M. E. Kerr, D. M. Ho, R. C. Elder, A. E. Bruce and M. R. M. Bruce, *Inorg. Chem.*, 1993, **32**, 2506.
18 M. N. I. Khan, J. P. Fackler, Jr., C. King, J. C. Wang and S. Wang, *Inorg. Chem.*, 1988, **27**, 1672.
19 S. D. Hanna, S. I. Khan and J. I. Zink, *Inorg. Chem.*, 1996, **35**, 5813.
20 S. Paulson, B. P. Sullivan and J. V. Caspar, *J. Am. Chem. Soc.*, 1992, **114**, 6905.
21 V. W.-W. Yam, C.-L. Chan and K.-K. Cheung, *J. Chem. Soc.*, *Dalton Trans.*, 1996, 4019.
22 J.-P. Collin, I. M. Dixon, J.-P. Sauvage and J. A. G. Williams, *J. Am. Chem. Soc.*, 1999, **121**, 5009.
23 L. J. Larson, E. M. McCauley, B. Weissbart and D. S. Tinti, *J. Phys. Chem.*, 1995, **99**, 7218.
24 E. M. Kober, J. L. Marshell, W. J. Dressick, B. P. Sullivan, J. V. Caspar and T. J. Meyer, *Inorg. Chem.*, 1985, **24**, 2755.
25 B. J. Pankuch, D. E. Lacky and G. A. Crosby, *J. Phys. Chem.*, 1980, **84**, 2061.
26 C. K. Johnson, ORTEP II, Report ORNL-5138, Oak Ridge National Laboratory, Oak Ridge, TN, 1976.
27 I. Schröter and J. Strähle, *Chem. Ber.*, 1991, **124**, 2161.
28 J. Vicente, M.-T. Chicote, P. González-Herrero and P. G. Jones, *J. Chem. Soc.*, *Dalton Trans.*, 1994, 3183.
29 D. J. LeBlanc, R. W. Smith, Z. Wang, H. E. Howard-Lock and C. J. L. Lock, *J. Chem. Soc.*, *Dalton Trans.*, 1997, 3263.
30 H. Nöth, W. Beck and K. Burger, *Eur. J. Inorg. Chem.*, 1998, 93.
31 R. Cea-Olivares, O. Jiménez-Sandoval, S. Hernández-Ortega, M. Sandez, R. A. Toscano and I. Haiduc, *Heteroat. Chem.*, 1995, **6**, 89.
32 P. Braunstein and R. J. H. Clark, *J. Chem. Soc.*, *Dalton Trans.*, 1973, 1845.
33 G. A. Bowmaker and B. C. Dobson, *J. Chem. Soc.*, *Dalton Trans.*, 1981, 267.
34 SIR 92; A. Altomare, M. C. Burla, M. Camalli, M. Cascarano, C. Giacovazzo, A. Guagliardi and G. Polidori, *J. Appl. Crystallogr.*, 1994, **27**, 435.
35 DIRDIF 94; P. T. Beurskens, G. Admiraal, W. P. Bosman, R. de Gelder, R. Israel and J. M. M. Smits. The DIRDIF 94 program system, Technical Report of the Crystallography Laboratory, University of Nijmegen, 1994.
36 TEXSAN, Molecular Structure Corporation, Houston, TX, 1985.